Surface Science 610 (2013) 65–69

Contents lists available at SciVerse ScienceDirect

Surface Science

journal homepage: www.elsevier.com/locate/susc

Self-organized Gd atomic superlattice on Ag(111): Scanning tunneling microscopy and kinetic Monte Carlo simulations

R.X. Cao, X.P. Zhang, B.F. Miao, Z.F. Zhong, L. Sun, B. You, An Hu, H.F. Ding *

National Laboratory of Solid State Microstructures and Department of Physics, Nanjing University, 22 Hankou Road, Nanjing 210093, PR China

ARTICLE INFO

Article history:
Received 27 November 2012
Accepted 18 January 2013
Available online 27 January 2013

Keywords:
Self organization
Long-range interaction
Scanning tunneling microscopy
Kinetic Monte Carlo simulations

ABSTRACT

With scanning tunneling microscopy, we experimentally demonstrate the self-organized Gd atomic superlattice on Ag(111) surface at low temperature. The diffusion barrier of a single Gd adatom and the long-range interaction between Gd adatoms on Ag(111) are determined. With these parameters, the formation mechanism is discussed and we confirm the validity of the previous discussed preconditions for formation of a good superlattice. The well-ordered structure is reproduced by the kinetic Monte Carlo simulations with the experimentally determined parameters. As well-ordered superlattice is realized in two different lanthanide adatoms on Ag(111), we predict that similar self-organization could form in other lanthanide adatoms because of their identical electron configuration in the outer shell and similar atomic radii.

1. Introduction

Ordered arrays of magnetic nanostructures are of special interests due to their rich physical properties and potential applications such as magnetic data storage. With the advance of modern growth and imaging techniques, it is possible to fabricate structures and investigate their unique properties down to the atomic level. Atom manipulation through scanning tunneling microscopy (STM) [1–6] and self-assembly growth [7–14] are two main routes to fabricate the atomic-scale structures. Atom manipulation is of advantage in building structures in arbitrary geometry. While self-assembly can provide well-ordered structures with relatively large area homogeneity and in an economic way. Self assembly through substrate mediated long-range interactions (LRI) between adatoms on noble metal (111) surfaces represents one of these typical samples [12,13,15,16]. The LRI was first predicted 50 years ago [17] and was revealed to oscillate with a periodicity of half the Fermi wavelength and decay with increasing the interatomic distance [18–20]. Hyldgaard and Persson investigated the LRI on the noble metal surface through Shockley surface states [21]. The LRI has a slower decay when the surface consists of a free electron-like surface state band. In addition, the wavelength of surface states at the Fermi level is generally longer than that of bulk states. Therefore, it is easier to be observed experimentally in the presence of surface state band. The LRI induced by surface states on Ag(111) and Cu(111) was indeed found by low-temperature STM [12,15,16,22]. On Cu/Cu(111) and Co/Cu(111), locally ordered structures with six-fold symmetry were observed, while no superlattice was found. Well-ordered hexagonal superlattice driven by the LRI was experimentally observed in Ce/Ag(111), Ce/Cu(111) and Fe/Cu(111) [12,22,23]. Former studies suggested that the formation mechanism for the self-organization is associated with the ratio of the first minimum of the LRI versus the diffusion barrier, and the ratio between the positions of the first minimum and first maximum of the LRI [23,24]. Zhang et al., further summarized these results into two empirical preconditions for forming the good superlattice [23]. It would be interesting to explore whether there are other systems that can form well-ordered superlattice. Particularly, the empirical preconditions need to be examined for new systems to prove their validity.

In this paper we report on the realization of the hexagonal superlattice for Gd adatoms on Ag(111) surfaces. At a coverage of 8.0×10^{-3} monolayer equivalent (MLE), the hexagonal superlattice with a periodicity of 3.0 nm is observed. Utilizing the experimentally determined diffusion barrier of a single Gd adatom and the LRI between Gd adatoms on Ag(111), we find that the two preconditions for forming a good superlattice discussed previously [23] are fulfilled in this new system. Furthermore, the kinetic Monte Carlo (KMC) simulations are performed and the results agree well with the experimental findings.

2. Experimental techniques

The experiments are performed in an ultrahigh vacuum chamber equipped with a low-temperature STM and a sputter gun. The base pressure is 2.0×10^{-11} mbar. The single-crystal substrate Ag(111) is cleaned by repeated cycles of argon ion sputtering (at 1.5 keV) and annealing (at 870 K). After that, the crystal is transferred into the STM stage and cooled to 4.7 K. The clean surface with low impurity concentration is checked by STM. The sample can be cooled further to 3.5 K by pumping liquid He in the cryostat. High purity Gd is deposited by means of electron beam evaporation onto the Ag(111)

* Corresponding author. Tel.: +86 25 8359 3795; fax: +86 25 8359 5535.
E-mail address: hfding@nju.edu.cn (H.F. Ding).

0039-6028/$ – see front matter © 2013 Elsevier B.V. All rights reserved.
http://dx.doi.org/10.1016/j.susc.2013.01.008

substrate in the STM stage at 6.0 K from the outgassed rod with a typical deposition rate of 0.002 monolayer/min. Electrochemically etched tungsten tips are used for the STM measurements. The bias voltage, U, refers to the sample voltage with respect to the tip.

3. Method of calculation

Kinetic Monte Carlo calculations are used to simulate the novel atomic structures of Gd on Ag(111) according to the experimental details. The method has been used previously for the simulation of the Fe superlattice formation on Cu(111) [23,25]. In the simulations, the hopping rate of an adatom from site i to site j on the Ag(111) surface is calculated using the Arrhenius law $\upsilon_{i\to j}=\upsilon_0\exp(-E_{i\to j}/k_BT)$, where T is the temperature of the substrate, υ_0 is the attempt frequency, k_B is the Boltzmann constant, and $E_{i\to j}$ is the hopping barrier. The influence of the LRI through the surface-state electrons is included in the hopping barrier, i.e., $E_{i\to j}=E_d+0.5(E_j-E_i)$ [26,27], where E_d is the diffusion barrier for an isolated atom on a clean surface, and $E_i(E_j)$ is the total energy caused by the LRI. The values of E_d and $E_i(E_j)$ are determined by experimental data which will be described below. To include the screening effect due to the dense packing, a cutoff radius of 4.1 nm is used which is similar to Ce/Ag(111) [24].

4. Results and discussion

Fig. 1(a) shows the typical image for 8.0×10^{-3} MLE Gd on Ag(111) obtained at 3.5 K. The scanning conditions are $U=-100$ mV and $I_t=2$ pA. We find Gd atoms form a well-ordered hexagonal superlattice except a few brighter spots. The brighter spots are dimers or trimers that form during deposition and have much higher diffusion barriers than a single Gd atom. Therefore, they are anchored once formed and they may not be at the ideal positions. The Fourier transform of the STM image shows a good hexagonal pattern [Inset of Fig. 1(a)] with the visible second order diffraction pattern. To obtain the statistical information, we plot in Fig. 1(b), the histogram of the nearest-neighbor Gd separation derived from the STM image shown in Fig. 1(a). It shows a sharp peak around 3.0 nm. For a comparison, the random distribution function with the same coverage is plotted as the solid line in Fig. 1(b) using the formula given by Knorr et al. [16] The peak appears at a different position and the random distribution function is much broader than the experimental histogram. These demonstrate that Gd adatoms with adequate coverage can form a well-ordered hexagonal superlattice on Ag(111).

In our previous study, we showed two empirical preconditions for forming a good superlattice. First, the ratio of the interaction energy E_i versus the diffusion barrier E_d needs to be larger than 5%. Second, the square of the specific value between the repulsive ring radius versus the superstructure lattice constant needs to be smaller than 19% [23]. The repulsive ring radius refers to the position where the LRI has absolute maximum energy, i.e., the first maximum energy position [27]. The definition is the same as in Ref. [23]. The physical picture can be understood as follows. Upon deposition, the atoms are randomly distributed. In order to form an ordered superlattice, they need to make enough steps to hop to the ideal positions with small thermal broadening. The effect of the thermal broadening is determined by the ratio of the depth of the potential well versus the temperature, which is proportional to the interaction energy versus the diffusion barrier. The higher the ratio is, the less the thermal broadening and the better superlattice can be achieved. Therefore, the ratio is one of the critical parameters which determine the formation condition for the superlattice. The second precondition ensures low dimer/trimer concentration. Dimers/trimers have much higher diffusion barriers than a single Gd atom. Therefore, they are anchored once formed and they may not be at the ideal positions and this will distort the well-ordered superlattice. The specific values of 5% and 19% are empirically summarized from several experimental systems [23]. In the following, we will experimentally

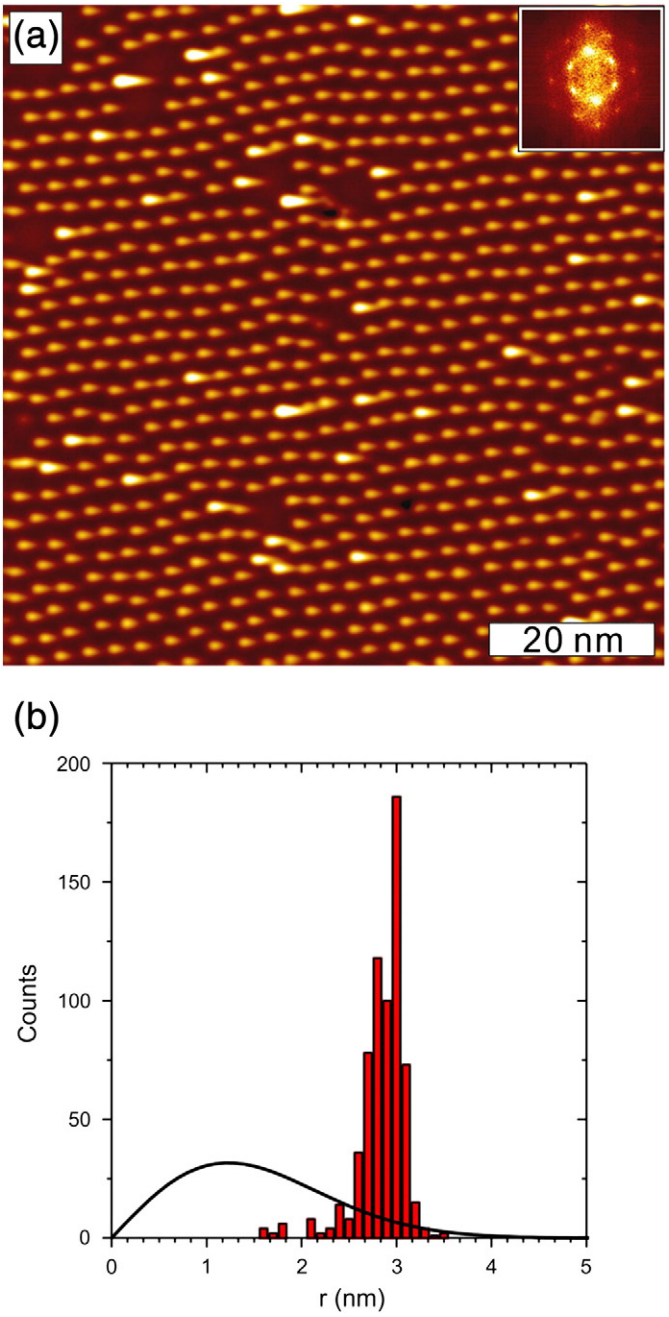

Fig. 1. (a) STM image of Gd superlattice on Ag(111) at 3.5 K (coverage $=8.0\times10^{-3}$ MLE, $U=-100$ mV and $I_t=2$ pA). Inset: Fourier transform of the image. (b) Histogram of the nearest-neighbor Gd separation obtained from (a) and the calculated random distribution with the same coverage (solid line).

measure these values for Gd on Ag(111) to check whether they fulfill the requirements mentioned above. The diffusion barrier and the attempt frequency of Gd on Ag(111) are obtained via the investigation of the atomic-diffusion process of single Gd atoms on a flat Ag(111) terrace, with the Gd atoms well separated from each other. We deposit 2.0×10^{-4} MLE Gd atoms on Ag(111) and cool down the sample to about 3.6 K. In such low temperature, the mobilities of the Gd adatoms are limited, allowing for the tracing of single-atom trajectories during STM imaging. We focus on a single Gd atom [Fig. 2(a)] and take consecutive scans of the same area with the rate of 10 s/frame. The scanning conditions are $U=-80$ mV and $I_t=2$ pA. No apparent tip-induced atom hopping is observed under this condition. In our analysis, we subtracted one image from its following image to check whether the

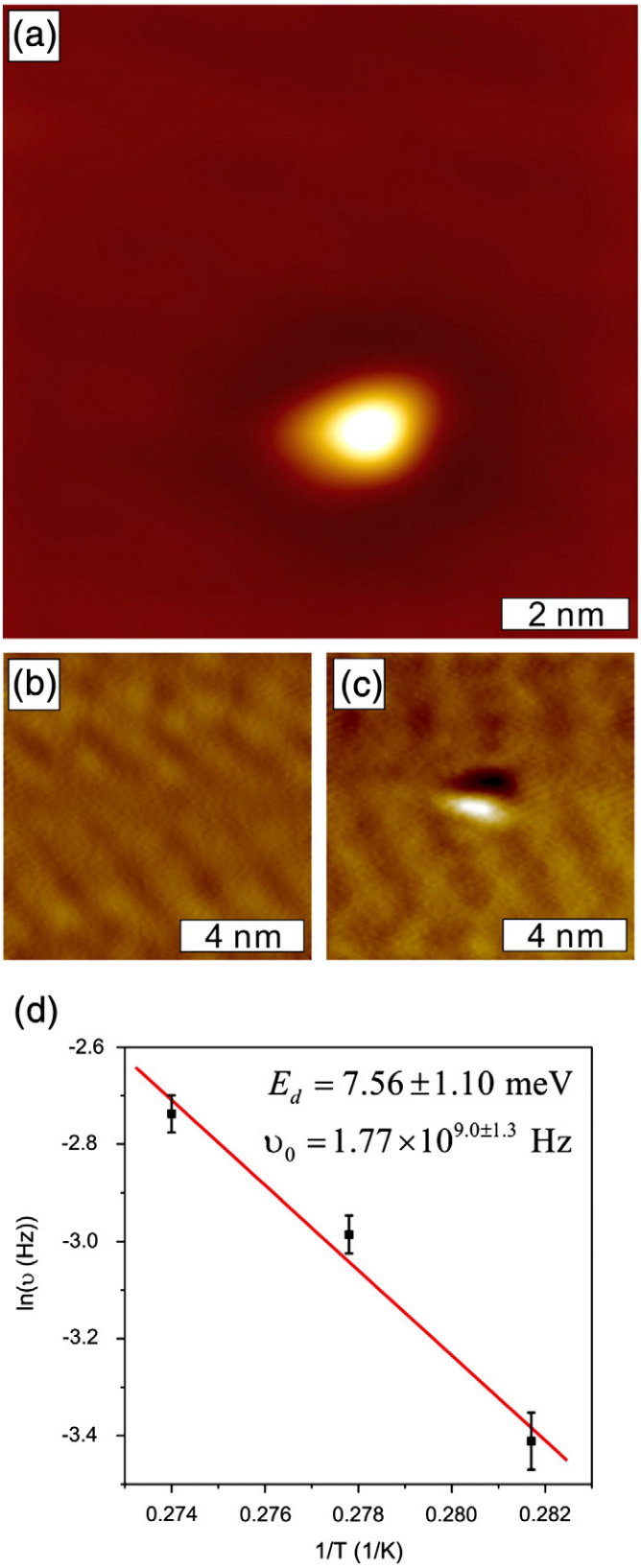

Fig. 2. (a) STM image of a single Gd atom at 3.6 K on Ag(111) ($U=-80$ mV and $I_t=2$ pA). (b) and (c) are typical images derived from subtraction of consecutive images like (a), which show no atomic diffusion and the downward atomic diffusion, respectively. (d) Arrhenius plot of the hopping rate of isolated Gd adatoms obtained from consecutive scans of (a) with the rate of 10 s/frame at different temperatures. The fitting yields the diffusion barrier and the attempt frequency.

adatom diffused or not. If the subtracted image shows no apparent contrast, as shown in Fig. 2(b), it stands for no moving of Gd adatom. On the contrary, if the subtracted image shows clear dark and bright contrast as in Fig. 2(c), it symbolizes that the adatom hopped. The hopping rates at different temperatures are recorded and used to fit with the Arrhenius law $\upsilon=\upsilon_0 \exp(-E_d/k_BT)$ [Fig. 2(d)]. The fitting yields the values of the diffusion barrier, $E_d=7.6\pm1.1$ meV, and the attempt frequency, $\upsilon_0=1.8\times10^{9.0\pm1.3}$ Hz. The value of diffusion barrier is similar to Ce/Ag(111) [12,28] and is lower than that of Fe/Cu(111) [23,29]. This may be related to their larger atomic radii compared to Fe adatom.

To measure the LRI between Gd adatoms, we deposit 2.0×10^{-3} MLE Gd single adatoms onto the Ag(111) surface. Through imaging the same area on a wide silver terrace at 4.0 K [Fig. 3(a)], we obtain a statistical histogram $f(r)$ of the nearest-neighbor Gd separation [red column in Fig. 3(b)]. The random distribution function $f_{ran}(r)$ of the same coverage [black curve in Fig. 3(b)] is also obtained and it is clearly different from the experimental histogram. With these, we can calculate the Gd–Gd LRI according to Boltzmann's statistics: $E(r)=-k_BT\ln[f(r)/f_{ran}(r)]$. The calculated LRI is shown as black dots in Fig. 3(c). The red curve is the fitting utilizing the theoretical model of the interactions between two adatoms mediated by a Shockley surface-state band [21], namely:

$$E(r) = -AE_0[2\sin(\delta_0)/\pi]^2 \times \sin(2k_Fr + 2\delta_0)/(k_Fr)^2 \quad (1)$$

where A is a scattering amplitude describing the scattering process from surface into bulk states, E_0 is the surface-state band edge (-67 meV) for Ag(111) [30], k_F is the Fermi wave vector (0.83 nm^{-1}) of the surface state [16], and δ_0 is the phase shift of scattering. The fitting yields $A=0.13\pm0.02$ and $\delta_0=(0.43\pm0.02)\pi$, which is close to the value $\delta_0=(0.37\pm0.05)\pi$ for Ce/Ag(111) [12,28]. It has the deepest minimum at 2.9 ± 0.1 nm and oscillation period of $\lambda_F/2=3.8$ nm, where λ_F is the Fermi wavelength of Ag(111) surface state. As the energy minimum of the LRI for Gd/Ag(111) appears at 2.9 nm, we can calculate the optimum coverage for the superlattice to be 1.0×10^{-2} MLE which is close to that in Fig. 1(a). We note that after Gd deposition at 6.0 K it takes a few minutes for cooling sample, so several ordered structures are even formed due to the high mobility of Gd atom at this temperature [Fig. 3(a)]. Therefore, many-body effect is inevitably included in the statistics and slight deviation from two-body model is expected. Besides, other effects may also play their roles in the discrepancy between the experimental data and the theoretical curve. When the Gd adtoms are landed on the Ag surface, they create certain strain on the substrate and may slightly change the long range interaction. In addition, it was reported that the LRI can have certain angular dependence [31]. The angularly averaged data can behave differently with the analytical calculations [32].

According to the LRI measurement, the depth of the first energy minimum E_i is about 0.6 meV and the ratio of E_i/E_d is 8% which satisfies the basic requirement of $>5\%$ for the self-organized superlattice formation [23]. Next we will check the second precondition. From the distance dependent LRI measurements, it is difficult to obtain the repulsive ring radius directly. In previous studies on Fe/Cu(111) and Ce/Ag(111) systems, the dimer concentration at low coverage is closely related to the square of the specific value between the repulsive ring radius versus the superstructure lattice constant. Therefore, we also use this method to estimate the radius of the repulsive ring for Gd adatoms on Ag(111). We count the concentration of the dimers among the Gd adatoms deposited and find it is about 6.4% at the coverage of 8.0×10^{-3} MLE. By assuming they are purely formed during the random deposition process, the repulsive ring radius is estimated to be ~0.8 nm. One should keep in mind that the requirement of the second precondition is to minimize the dimer concentration. The experimentally determined 6.4% concentration of dimer is also much smaller than the value of 19% which was estimated to be the upper limit of forming good superlattice [23]. Therefore, the two preconditions

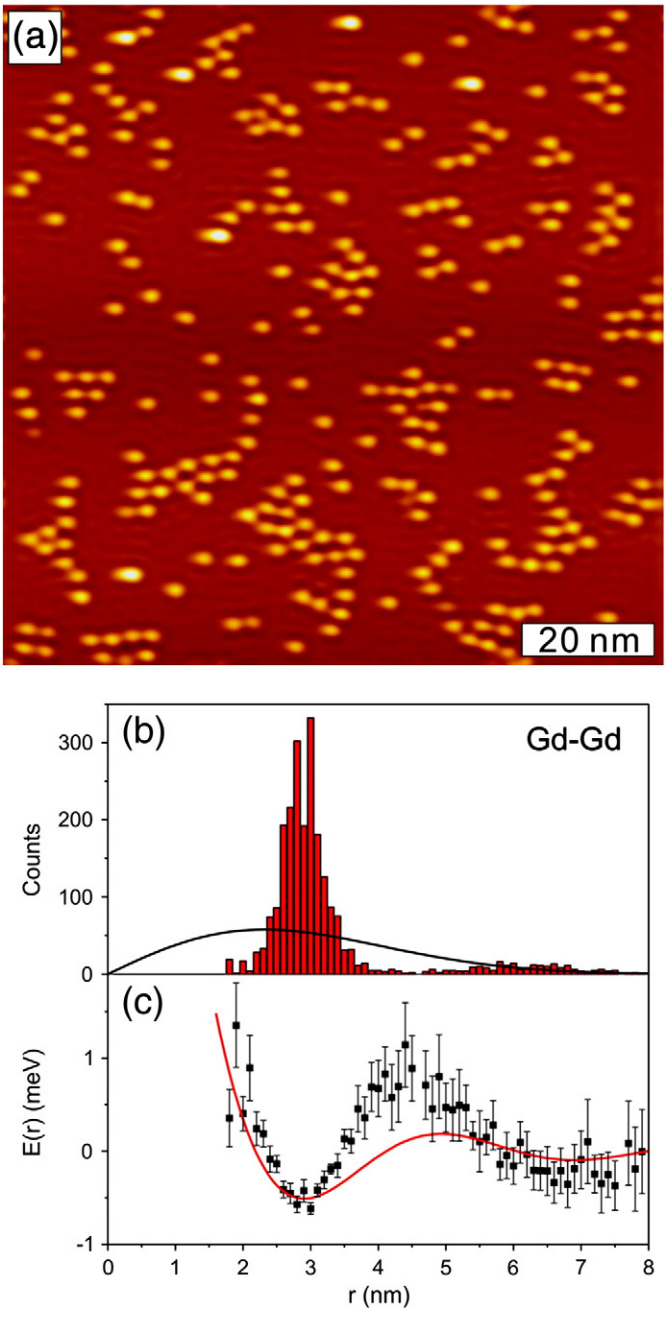

Fig. 3. (a) STM image of 2.0×10^{-3} MLE Gd atoms on Ag(111) at 4.0 K. (b) Histogram of the nearest-neighbor Gd separation obtained from (a) and the calculated random distribution (black line). (c) Long-range interaction between two Gd atoms derived from (b) (black dots) and fitting using Eq. (1) (red line).

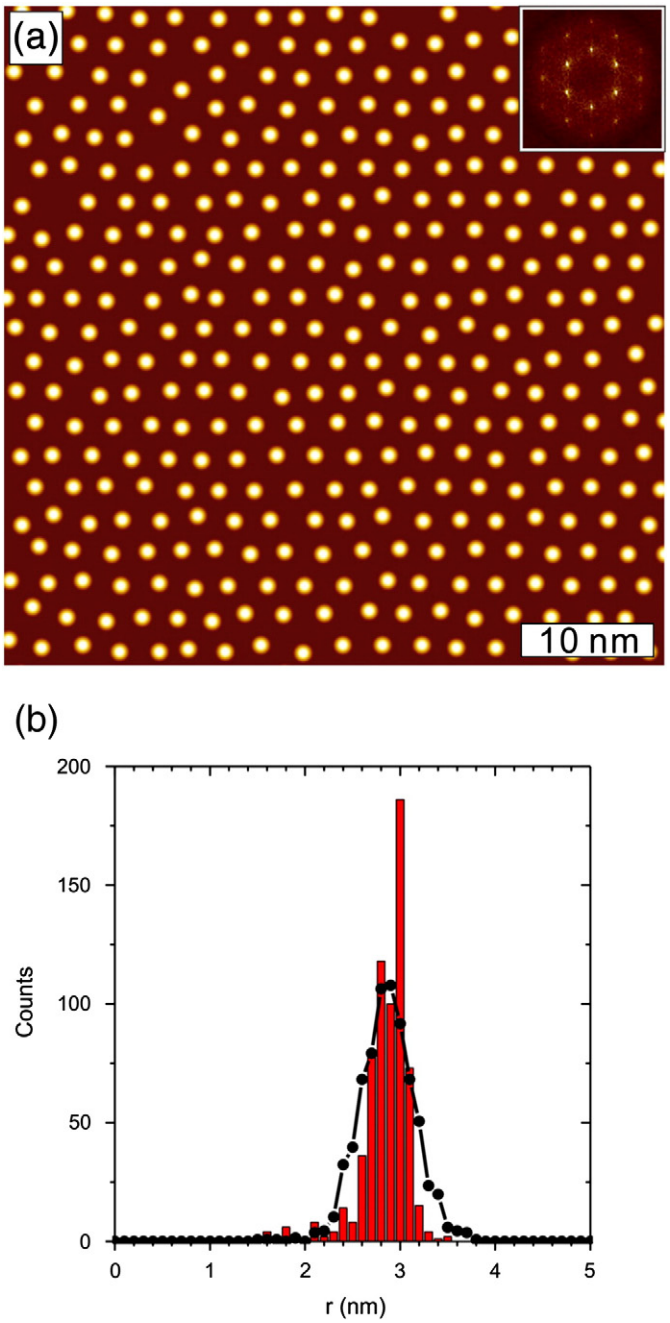

Fig. 4. (a) Kinetic Monte Carlo simulations for 1.0×10^{-2} MLE Gd/Ag(111). Inset: Fourier transform of the image. (b) The comparison of the nearest-neighbor separation distribution between KMC simulations (black circles) and experiment [red column same as Fig. 1(b)]. The KMC results are normalized to experimental results according to their different image sizes.

mentioned above are fulfilled in Gd/Ag(111) system, in good support for the conclusion in Ref. [23].

With the diffusion barrier and the interaction energy obtained experimentally, we further perform the KMC simulations for Gd/Ag(111) at the optimal coverage with the method described in Section 3. Fig. 4(a) presents the simulated results at 3.5 K and it indeed shows an almost perfect superlattice with the lattice constant of 3.0 nm. The quality of the superlattice can also be confirmed by the Fourier transform image, which shows a sharp hexagonal pattern with clearly visible second-order diffraction spots [Inset of Fig. 4(a)]. We plot in Fig. 4(b) as black circles, the distribution of the nearest-neighbor Gd separation derived from Fig. 4(a). Comparing with experimental results [red column same as Fig. 1(b)], the preferred separation 3.0 nm and the similar peak width are obtained. These illustrate that the simulations agree well with the experiments. We note that the dimers/trimers formation was neglected in the KMC simulations due to their low concentration.

Well-ordered hexagonal superlattice is realized in both Gd/Ag(111) and Ce/Ag(111) systems [12,28]. This could be extrapolated to the group of Lanthanides since both Gd and Ce are Lanthanides. As discussed above and in Ref. [23], there are two preconditions for forming good superlattice, the ratio between the LRI and the diffusion barrier, and the ratio between the positions of the first minimum and first maximum of the LRI. These two systems show quite similar LRI (0.6 and 0.8 meV) and diffusion barrier (7.6 and 10 meV). As the long range interaction intrinsically is the Coulomb interaction, it should be mainly determined by

the outer shell electrons. Lanthanides have identical outer shell electron configuration. It would be expected they have similar long range interaction on the same surface, Ag(111). It is also expected that they have almost the same interactions with the Ag substrate. In addition, their atomic radii are close to each other, varying from 0.173 to 0.204 nm only. Thus, they may have similar diffusion barriers on Ag(111). Therefore, we speculate that the group of Lanthanides may form good superlattice on Ag(111). It would be interesting to further verify this experimentally.

5. Summary

In summary, we experimentally demonstrate the formation of Gd hexagonal superlattice on Ag(111) surfaces. Quantitative analysis reveals that the nearest-neighbor Gd separation is about 3.0 nm. The diffusion barrier of a single Gd atom and the LRI between Gd atoms on Ag(111) are obtained experimentally. The two preconditions for forming good superlattice raised by Ref. [23] are examined for Gd/Ag(111) system and good agreement is found. The KMC simulations are performed utilizing the experimentally determined parameters and the result agrees well with the experiments. As well-ordered superlattice is realized in both Gd/Ag(111) and Ce/Ag(111) systems, similar self-organization could form in other lanthanide adatoms on Ag(111) because of their identical electron configuration in the outer shell and similar atomic radii.

Acknowledgments

This work is supported by the State Key Program for Basic Research of China (Grant No. 2010CB923401), NSFC (Grants Nos. 10834001, 10974087, and 11023002) and PAPD.

References

[1] D.M. Eigler, E.K. Schweizer, Nature 344 (1990) 524.
[2] M.F. Crommie, C.P. Lutz, D.M. Eigler, Science 262 (1993) 218.
[3] H.C. Manoharan, C.P. Lutz, D.M. Eigler, Nature 403 (2000) 512.
[4] N. Nilius, T.M. Wallis, W. Ho, Science 297 (2002) 1853.
[5] C.F. Hirjibehedin, C.P. Lutz, A.J. Heinrich, Science 312 (2006) 1021.
[6] S. Loth, S. Baumann, C.P. Lutz, D.M. Eigler, A.J. Heinrich, Science 335 (2012) 196.
[7] D.D. Chambliss, R.J. Wilson, S. Chiang, Phys. Rev. Lett. 66 (1991) 1721.
[8] H. Brune, M. Giovannini, K. Bromann, K. Kern, Nature 394 (1998) 451.
[9] S. Sun, C.B. Murray, D. Weller, L. Folks, A. Moser, Science 287 (2000) 1989.
[10] G.M. Whitesides, B. Grzybowski, Science 295 (2002) 2418.
[11] P. Gambardella, A. Dallmeyer, K. Maiti, M.C. Malagoli, W. Eberhardt, K. Kern, C. Carbone, Nature 416 (2002) 301.
[12] F. Silly, M. Pivetta, M. Ternes, F. Patthey, J.P. Pelz, W.-D. Schneider, Phys. Rev. Lett. 92 (2004) 016101.
[13] H.F. Ding, V.S. Stepanyuk, P.A. Ignatiev, N.N. Negulyaev, L. Niebergall, M. Wasniowska, C.L. Gao, P. Bruno, J. Kirschner, Phys. Rev. B 76 (2007) 033409.
[14] N. Nilius, E.D.L. Rienks, H.-P. Rust, H.-J. Freund, Phys. Rev. Lett. 95 (2005) 066101.
[15] J. Repp, F. Moresco, G. Meyer, K.-H. Rieder, P. Hyldgaard, M. Persson, Phys. Rev. Lett. 85 (2000) 2981.
[16] N. Knorr, H. Brune, M. Epple, A. Hirstein, M.A. Schneider, K. Kern, Phys. Rev. B 65 (2002) 115420.
[17] J. Koutecký, Trans. Faraday Soc. 54 (1958) 1038.
[18] T.B. Grimley, Proc. Phys. Soc. 90 (1967) 751.
[19] T.L. Einstein, J.R. Schrieffer, Phys. Rev. B 7 (1973) 3629.
[20] K.H. Lau, W. Kohn, Surf. Sci. 75 (1978) 69.
[21] P. Hyldgaard, M. Persson, J. Phys. Condens. Matter 12 (2000) L13.
[22] N.N. Negulyaev, V.S. Stepanyuk, L. Niebergall, P. Bruno, M. Pivetta, M. Ternes, F. Patthey, W.D. Schneider, Phys. Rev. Lett. 102 (2009) 246102.
[23] X.P. Zhang, B.F. Miao, L. Sun, C.L. Gao, A. Hu, H.F. Ding, J. Kirschner, Phys. Rev. B 81 (2010) 125438.
[24] N.N. Negulyaev, V.S. Stepanyuk, L. Niebergall, W. Hergert, H. Fangohr, P. Bruno, Phys. Rev. B 74 (2006) 035421.
[25] J. Hu, B. Teng, F. Wu, Y. Fang, New J. Phys. 10 (2008) 023033.
[26] K.A. Fichthorn, W.H. Weinberg, Phys. Rev. Lett. 68 (1992) 604.
[27] K.A. Fichthorn, M. Scheffler, Phys. Rev. Lett. 84 (2000) 5371.
[28] F. Silly, M. Pivetta, M. Ternes, F. Patthey, J.P. Pelz, W.-D. Schneider, New J. Phys. 6 (2004) 16.
[29] N.N. Negulyaev, V.S. Stepanyuk, L. Niebergall, P. Bruno, W. Auwarter, Y. Pennec, G. Jahnz, J.V. Barth, Phys. Rev. B 79 (2009) 195411.
[30] J. Li, W.-D. Schneider, R. Berndt, Phys. Rev. B 56 (1997) 7656.
[31] W. Luo, K.A. Fichthorn, Phys. Rev. B 72 (2005) 115433.
[32] J.D. Howe, P. Bhopale, Y. Tiwary, K.A. Fichthorn, Phys. Rev. B 81 (2010) 121410.